JACS
JOURNAL OF THE AMERICAN CHEMICAL SOCIETY

ARTICLE

pubs.acs.org/JACS

Insertion, Isomerization, and Cascade Reactivity of the Tethered Silylalkyl Uranium Metallocene $(\eta^5\text{-}C_5Me_4SiMe_2CH_2\text{-}\kappa C)_2U$

Nathan A. Siladke, Joseph W. Ziller, and William J. Evans*

Department of Chemistry, University of California, Irvine, California 92697-2025, United States

Supporting Information

ABSTRACT: Investigation of the insertion reactivity of the tethered silylalkyl complex $(\eta^5\text{-}C_5Me_4SiMe_2CH_2\text{-}\kappa C)_2U$ (**1**) has led to a series of new reactions for U−C bonds. Elemental sulfur reacts with **1** by inserting two sulfur atoms into each of the U−C bonds to form the bis(tethered alkyl disulfide) complex $(\eta^5\text{:}\eta^2\text{-}C_5Me_4SiMe_2CH_2S_2)_2U$ (**2**). The bulky substrate *N*,*N*′-diisopropylcarbodiimide, ^{i}PrN═C═N^{i}Pr, inserts into only one of the U−C bonds of **1** to produce the mixed-tether complex $(\eta^5\text{-}C_5Me_4SiMe_2CH_2\text{-}\kappa C)U[\eta^5\text{-}C_5Me_4SiMe_2CH_2C(^i PrN)_2\text{-}\kappa^2N,N']$ (**3**). Carbon monoxide did not exclusively undergo a simple insertion into the U−C bond of **3** but instead formed $\{\mu\text{-}[\eta^5\text{-}C_5Me_4SiMe_2CH_2C(=N^iPr)O\text{-}\kappa^2O,N]U[OC(C_5Me_4SiMe_2CH_2)CN(^iPr)\text{-}\kappa^2O,N]_2$ (**4**) in a cascade of reactions that formally includes U−C bond cleavage, C−N bond cleavage of the amidinate ligand, alkyl or silyl migration, U−O, C−C, and C−N bond formations, and CO insertion. The reaction of **3** with isoelectronic *tert*-butyl isocyanide led to insertion of the substrate into the U−C bond, but with a rearrangement of the amidinate ligand binding mode from κ^2 to κ^1 to form $[\eta^5\text{:}\eta^2\text{-}C_5Me_4SiMe_2CH_2C(=N^tBu)]U[\eta^5\text{-}C_5Me_4SiMe_2CH_2C(=N^iPr)N(^iPr)\text{-}\kappa N]$ (**5**). The product of double insertion of ^{t}BuN≡C into the U−C bonds of **1**, namely $[\eta^5\text{:}\eta^2\text{-}C_5Me_4SiMe_2CH_2C(=N^tBu)]_2U$ (**6**), was found to undergo an unusual thermal rearrangement that formally involves C−H bond activation, C−C bond cleavage, and C−C bond coupling to form the first formimidoyl actinide complex, $[\eta^5\text{:}\eta^5\text{:}\eta^3\text{-}^tBuNC(CH_2SiMe_2C_5Me_4)(CHSiMe_2C_5Me_4)]U(\eta^2\text{-}HC=N^tBu)$ (**7**).

INTRODUCTION

Insertion reactions constitute one of the central transformations in organometallic chemistry and are often critical steps in various types of catalytic transformations.[1−4] One general approach to a detailed investigation of insertion reactivity of metal complexes is to tether the reactive site to another ligand in the complex in order to gain greater control of the parameters in the reaction. Although this method has been widely applied to the study of transition-metal complexes,[5−7] it has seldom been utilized with organoactinides despite the broad interest of insertion into actinide−element bonds and the relevance to catalysis.[8,9]

Recent studies have led to the isolation of $(\eta^5\text{-}C_5Me_4SiMe_2CH_2\text{-}\kappa C)_2U$ (**1**), an unusual complex containing two reactive alkyl ligands tethered by the ancillary ligands to a single metal center.[10] Preliminary reactivity studies of **1** with carbon monoxide and *tert*-butyl isocyanide (eq 1) have demonstrated that this system can provide insertion product structural data that are not accessible with the nontethered analogue, namely $(C_5Me_5)_2UMe_2$.[10,11] In addition, each time **1** participates in an insertion reaction, a new tethered metallocene is formed, allowing further exploration of uranium−element bond reactivity in a tethered environment.

We report here a series of new reactivity options for U−C bonds using tethered complexes of the type shown in eq 1. Insertion chemistry with elemental sulfur and a carbodiimide, unexpected cascade and rearrangement reactivity with the carbodiimide insertion product, and an unusual isomerization of a bis(iminoacyl) complex involving C−C and C−H bond activation are reported.

(1)

The reaction of **1** with elemental sulfur was examined to expand options for the synthesis of actinide sulfur compounds. Actinide sulfides are of interest, since it has been shown that selective complexation of actinides versus lanthanides, useful in nuclear waste separation, is facilitated by soft ligands for the actinides.[12,13] Despite the potential of An−S systems as soft alternatives to the oxygen donor ligand chemistry that predominates with these oxophilic metals, only recently has a report on U−S bond formation directly from elemental sulfur appeared.[14]

Received: October 21, 2010
Published: February 18, 2011

dx.doi.org/10.1021/ja109491k | *J. Am. Chem. Soc.* 2011, 133, 3507–3516

The reaction of **1** with *N,N′*-diisopropylcarbodiimide was explored to test the limits of insertion reactivity of sterically bulky substrates. Although alkyl isocyanides can insert into both of the U−C bonds of **1** (eq 1), this seemed unlikely with a large substrate such as ^{i}PrN═C═N^{i}Pr. Single insertion of ^{i}PrN═C═N^{i}Pr with $(C_5Me_5)_2UMe_2$ has been previously observed.[15] If a single insertion occurred with **1**, this would provide a complex with two different types of tethers. Such complexes allow comparative studies of reactivity between different tethered ligands in the same molecule as reported here for CO.

The thermal stability of the bis(tethered iminoacyl) complex shown in eq 1, $[\eta^5{:}\eta^2\text{-}C_5Me_4SiMe_2CH_2C(=N^tBu)]_2U$ (**6**), was examined for comparison with bis(iminoacyl) transition-metal complexes that undergo C−C coupling of the iminoacyl ligands upon heating[16] (eq 2).[17] Since C−C bond formation constitutes an important step in many chemical transformations and complex **6** is the only bis(iminoacyl) f element compound known, it provided the first opportunity to evaluate this type of reaction.

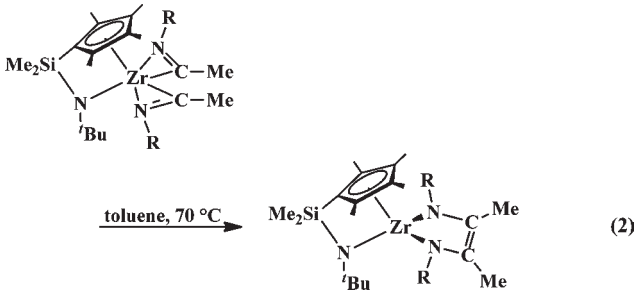

(2)

EXPERIMENTAL SECTION

The syntheses and manipulations described below were conducted under argon or nitrogen with rigorous exclusion of air and water using glovebox, Schlenk, and vacuum-line techniques. All reactions were performed at room temperature unless otherwise noted. Solvents were dried over columns containing Q-5 and 4A molecular sieves. Benzene-d_6 and toluene-d_8 were dried over sodium−potassium alloy, degassed using three freeze−pump−thaw cycles, and vacuum-transferred before use. *tert*-Butyl isocyanide and *N,N′*-diisopropylcarbodiimide were dried over 4A molecular sieves and degassed using three freeze−pump−thaw cycles before use. S_8 was purchased from Aldrich and purified by sublimation before use. Ultrahigh-purity carbon monoxide was purchased from Airgas and used as received. $(\eta^5\text{-}C_5Me_4SiMe_2CH_2\text{-}\kappa C)_2U$ (**1**) and $[\eta^5{:}\eta^2\text{-}C_5Me_4SiMe_2CH_2C(=N^tBu)]_2U$ (**6**) were prepared as previously reported.[10] NMR spectra were recorded with a Bruker DRX 500 MHz spectrometer or a Bruker CRYO 500 MHz spectrometer (^{13}C NMR recorded at 125 MHz) at room temperature, except where noted. Due to the paramagnetism of uranium, only resonances that could be unambiguously identified are reported. Infrared spectra were recorded as KBr pellets on a Varian 1000 FT-IR spectrometer. Elemental analysis was performed on a Perkin-Elmer 2400 Series II CHNS analyzer.

$(\eta^5{:}\eta^2\text{-}C_5Me_4SiMe_2CH_2S_2)_2U$ (2). A solution of **1** (101 mg, 0.16 mmol) in toluene (10 mL) was added to a stirred slurry of S_8 (21 mg, 0.08 mmol) in toluene (3 mL). The orange solution was stirred for 45 min, and the solvent was removed under vacuum to yield an orange-brown solid. This solid was washed with hexane (3 mL) and dried under vacuum, yielding **2** as an orange microcrystalline solid (60 mg, 50%). X-ray-quality crystals of **2** were grown from hexane at −35 °C. Solutions of **2** decompose after 12 h at room temperature to give a black insoluble material. ^{1}H NMR (toluene-d_8, −45 °C): δ −37.5 (s, 2H, CH_2), −17.6 (s, 6H, C_5Me_4), −6.6 (s, 6H, C_5Me_4), 4.9 (s, 6H, SiMe_2), 5.0 (s, 6H, SiMe_2), 12.2 (s, 6H, C_5Me_4), 22.9 (s, 2H, CH_2), 25.9 (s, 6H, C_5Me_4). IR: 2945 s, 2903 s, 1486 w, 1446 w, 1378 m, 1351 w, 1328 m, 1246 m, 1133 w, 1103 w, 1021 w, 839 s, 827 m, 816 w, 789 m, 749 m, 687 w, 673 w, 632 w, 519 w cm^{-1}. Anal. Calcd for $C_{24}H_{40}Si_2S_4U$: C, 38.38; H, 5.37. Found: C, 39.12; H, 5.05. Due to the low solubility of concentrated samples of **2** at −45 °C, ^{13}C NMR was not obtained.

$(\eta^5\text{-}C_5Me_4SiMe_2CH_2\text{-}\kappa C)U[\eta^5\text{-}C_5Me_4SiMe_2CH_2C(^{i}PrN)_2\text{-}\kappa^2N,N']$ (3). A solution of ^{i}PrN═C═N^{i}Pr (76 μL, 0.49 mmol) in toluene (5 mL) was added to a stirred solution of **1** (306 mg, 0.49 mmol) in toluene (10 mL). The red solution was stirred for 12 h, and the solvent was removed under vacuum to yield **3** as a red-orange powder (360 mg, 98%). ^{1}H NMR (toluene-d_8, −45 °C): δ −27.5 (s, 3H, C_5Me_4), −24.7 (s, 3H, C_5Me_4), −24.4 (s, 3H, C_5Me_4), −23.4 (s, 1H, CH(Me)$_2$), −4.9 (s, 1H, CH(Me)$_2$), −4.1 (s, 3H, C_5Me_4), −2.3 (s, 3H, C_5Me_4), −0.4 (s, 3H, SiMe_2), 3.9 (s, 3H, SiMe_2), 6.3 (s, 3H, SiMe_2), 19.9 (d, $^2J_{HH}$ = 13 Hz, 1H, CH_2), 22.1 (s, 3H, C_5Me_4), 24.3 (s, 3H, CH(*Me*)$_2$), 24.8 (s, 3H, CH(*Me*)$_2$), 28.6 (s, 3H, C_5Me_4), 33.4 (s, 3H, C_5Me_4). IR: 2967 s, 2900 m, 2871 m, 1442 m, 1381 m, 1362 w, 1335 m, 1302 m, 1245 m, 1176 m, 1124 w, 1102 w, 1079 w, 1044 w, 1018 w, 838 s, 812 m, 766 m, 711 w, 679 m, 651 w cm^{-1}. Anal. Calcd for $C_{31}H_{54}N_2Si_2U$: C, 49.71; H, 7.23; N, 3.74. Found: C, 49.93; H, 7.88; N, 3.46. Due to the low solubility of concentrated samples of **3** at −45 °C, ^{13}C NMR was not obtained.

$\{\mu\text{-}[\eta^5\text{-}C_5Me_4SiMe_2CH_2C(=N^{i}Pr)O\text{-}\kappa^2O,N]U[OC(C_5Me_4SiMe_2CH_2)CN(^{i}Pr)\text{-}\kappa^2O,N]\}_2$ (4). A red solution of **3** (99 mg, 0.28 mmol) in benzene (15 mL) in a 100 mL Schlenk flask equipped with a Teflon stopper was attached to a high-vacuum line and degassed by three freeze−pump−thaw cycles. CO (1 atm) was introduced into the reaction flask at room temperature, and the solution was stirred. After 15 min, the solution turned brown-yellow, was degassed by a freeze−pump−thaw cycle, and was brought into an argon-filled glovebox. Removal of the solvent under vacuum yielded **4** as a brown powder (106 mg, 98%). X-ray-quality crystals of **4** were grown from hexane at −35 °C. ^{1}H NMR (C_6D_6): δ −44.1 (s, 3H, C_5Me_4), −42.7 (s, 3H, C_5Me_4), −37.4 (s, 1H, CHMe$_2$), −28.1 (s, 3H, C_5Me_4), −23.1 (s, 3H, C_5Me_4), −14.3 (s, 3H, CHMe$_2$), −12.6 (s, 3H, CHMe$_2$), −11.6 (d, $^2J_{HH}$ = 16 Hz, 1H, SiMe$_2$CH_2), −8.7 (s, 3H, CHMe$_2$), −7.4 (s, 3H, SiMe_2), 2.9 (s, 3H, SiMe_2), 5.9 (s, 3H, SiMe_2), 10.5 (s, 3H, SiMe_2), 12.5 (s, 3H, C_5Me_4), 19.7 (s, 3H, C_5Me_4), 20.9 (d, $^2J_{HH}$ = 16 Hz, 1H, SiMe$_2$CH_2), 25.3 (s, 3H, C_5Me_4), 29.6 (s, 3H, C_5Me_4), 47.0 (s, 1H, SiMe$_2$CH_2), 47.7 (s, 1H, SiMe$_2$CH_2), 69.3 (s, 3H, CHMe$_2$), 80.4 (s, 1H, CHMe$_2$). ^{13}C NMR (C_6D_6): δ −160.6 (SiMe$_2$CH$_2$), −129.8 (C_5Me_4), −113.2 (C_5Me_4), −102.0 (C_5Me_4), −71.4 (CHMe$_2$), −51.3 (CHMe$_2$), −45.9 (SiMe_2), −39.9 (SiMe_2), −19.6 (SiMe_2), −8.6 (CHMe$_2$), −5.0 (CHMe$_2$), 11.7 (SiMe_2), 13.9 (C_5Me_4), 20.2 (C_5Me_4), 21.5 (SiMe_2), 29.1 (C_5Me_4), 83.2 (SiMe$_2$CH$_2$), 97.7 (C_5Me_4), 112.0 (CHMe$_2$), 181.3 (CHMe$_2$). IR: 3071 w, 2963 s, 2907 s, 2865 s, 1575 m, 1439 m, 1381 m, 1362 w, 1322 m, 1301 w, 1247 m, 1192 m, 1177 m, 1125 w, 1103 w, 1077 w, 1047 w, 1018 w, 985 s, 907 w, 837 s, 810 m, 768 m, 729 w, 676 m, 635 w, 587 w, 460 s cm^{-1}. Anal. Calcd for $C_{66}H_{108}N_4O_4Si_4U_2$: C, 49.24; H, 6.76; N, 3.48. Found: C, 49.77; H, 6.75; N, 3.32.

$[\eta^5{:}\eta^2\text{-}C_5Me_4SiMe_2CH_2C(=N^tBu)]U[\eta^5\text{-}C_5Me_4SiMe_2CH_2C(=N^{i}Pr)N(^{i}Pr)\text{-}\kappa N]$ (5). A solution of ^{t}BuN≡C (44 μL, 0.39 mmol) in toluene (5 mL) was added to a stirred solution of **3** (68 mg, 0.19 mmol) in toluene (10 mL). After 12 h, no color change was observed, and the solvent was removed under vacuum to yield **5** as a red powder (76 mg, 99%). X-ray-quality crystals of **5** were grown from hexane at −35 °C. ^{1}H NMR (C_6D_6): δ −61.3 (s, 3H, C_5Me_4), −55.4 (s, 3H, C_5Me_4), −35.5 (s, 1H, CH_2), −33.6 (s, 3H, C_5Me_4), −32.9 (s, 3H, C_5Me_4), −19.5 (s, 9H, N^tBu), −6.8 (s, 3H, SiMe_2), 0.3 (s, 3H, SiMe_2), 3.5 (s, 1H, CH_2), 6.8 (s, 3H, SiMe_2), 13.0 (s, 3H, SiMe_2), 15.4 (s, 3H, C_5Me_4), 16.5 (s, 3H, C_5Me_4), 19.0 (s, 3H, C_5Me_4), 19.2 (s, 3H, C_5Me_4), 21.0 (d, $^3J_{HH}$ = 5 Hz, 3H, CH(*Me*)$_2$), 21.4 (d, $^3J_{HH}$ = 6 Hz, 3H, CH(*Me*)$_2$), 24.7 (s, 3H, CH(*Me*)$_2$), 31.1 (s, 3H, CH(*Me*)$_2$), 37.3 (s, 1H, CH_2), 45.0 (s, 1H, CH_2). ^{13}C NMR (C_6D_6): δ −166.0 (C_5Me_4), −127.0 (C_5Me_4), −90.9 (C_5Me_4), −86.7 (C_5Me_4), −36.9 (C_5Me_4), −25.9 (C_5Me_4), −21.9 (N^tBu), −1.0 (SiMe_2), −0.8 (SiMe_2), 4.6 (SiMe_2), 19.4 (C_5Me_4), 23.4 (CH(*Me*)$_2$), 26.0 (CH$_2$), 31.0 (CH(*Me*)$_2$), 59.4 (CH(*Me*)$_2$),

Table 1. X-ray Data Collection Parameters for $(\eta^5{:}\eta^2\text{-}C_5Me_4SiMe_2CH_2S_2)_2U$ (2), $\{\mu\text{-}[\eta^5\text{-}C_5Me_4SiMe_2CH_2C(=N^tPr)O\text{-}\kappa^2O,N]U[OC(C_5Me_4SiMe_2CH_2)CN(^iPr)\text{-}\kappa^2O,N]\}_2$ (4), $[\eta^5{:}\eta^2\text{-}C_5Me_4SiMe_2CH_2C(=N^tBu)]U[\eta^5\text{-}C_5Me_4SiMe_2CH_2C(=N^iPr)N(^tPr)\text{-}\kappa N]$ (5), and $[\eta^5{:}\eta^5{:}\eta^3\text{-}^tBuNC(CH_2SiMe_2C_5Me_4)(CHSiMe_2C_5Me_4)]U(\eta^2\text{-}HC{=}N^tBu)$ (7)

	2	4	5	7
empirical formula	$C_{24}H_{40}S_4Si_2U$	$C_{66}H_{108}N_4O_4Si_4U_2$	$C_{36}H_{63}N_3Si_2U$	$C_{34}H_{58}N_2Si_2U$
formula wt	751.01	1609.98	832.10	789.03
temp (K)	153(2)	148(2)	148(2)	153(2)
cryst syst	monoclinic	monoclinic	triclinic	monoclinic
space group	$C2/c$	$C2/c$	$P\bar{1}$	$P2_1/c$
a (Å)	19.6639(15)	14.9569(9)	10.8031(6)	10.0856(5)
b (Å)	8.7482(7)	19.1828(11)	12.6268(7)	17.4636(9)
c (Å)	17.1940(13)	27.7740(15)	14.8665(8)	19.6548(10)
α (deg)	90	90	92.1180(6)	90
β (deg)	108.5767(9)	95.2545(7)	91.9633(6)	104.7607(7)
γ (deg)	90	90	112.8823(5)	90
V (Å^3)	2803.7(4)	7078.2(7)	1864.45(18)	3347.6(3)
Z	4	4	2	4
ρ_{calcd} (Mg/m^3)	1.779	1.511	1.482	1.566
μ (mm^{-1})	6.185	4.683	4.444	4.945
R1[a] ($I > 2.0\sigma(I)$)	0.0162	0.0175	0.0158	0.0326
wR2[b] (all data)	0.0376	0.0444	0.0401	0.0744

[a] $R1 = \sum||F_o| - |F_c||/\sum|F_o|$. [b] $wR2 = [\sum[w(F_o^2 - F_c^2)^2]/\sum[w(F_o^2)^2]]^{1/2}$.

68.9 ($CH(Me)_2$), 73.7 ($SiMe_2$), 86.3 (C_5Me_4), 88.2 (CH_2). IR: 2959 s, 2913 s, 1649 w, 1581 vs, 1450 m, 1382 w, 1361 m, 1328 m, 1265 m, 1188 m, 1170 m, 1135 m, 1062 m, 1020 w, 994 m, 953 m, 884 m, 835 s, 757 w, 727 w, 690 w, 666 w cm^{-1}. Anal. Calcd for $C_{36}H_{63}N_3Si_2U$: C, 51.96; H, 7.63; N, 5.05. Found: C, 52.11; H, 7.90; N, 5.00.

$[\eta^5{:}\eta^5{:}\eta^3\text{-}^tBuNC(CH_2SiMe_2C_5Me_4)(CHSiMe_2C_5Me_4)]U(\eta^2\text{-}HC{=}N^tBu)$ (7). A red solution of $[\eta^5{:}\eta^2\text{-}C_5Me_4SiMe_2CH_2C(=N^tBu)]_2U$ (**6**; 125 mg, 0.16 mmol) in toluene (20 mL) was heated in a 100 mL side-arm Schlenk flask at 110 °C for 12 h, after which the solution became brown-red. The solvent was removed under vacuum, yielding a brown powder. X-ray-quality crystals of **7** were grown from toluene at −35 °C (69 mg, 55% crystalline). ^{1}H NMR (toluene-d_8): δ −51.8 (s, 3H, C_5Me_4), −51.2 (s, 3H, C_5Me_4), −41.8 (s, 3H, C_5Me_4), −34.6 (s, 3H, C_5Me_4), −10.0 (bs, 9H, N^tBu), −5.0 (s, 3H, $SiMe_2$), −3.9 (s, 9H, N^tBu), −3.6 (s, 3H, $SiMe_2$), 3.3 (s, 3H, $SiMe_2$), 4.9 (s, 3H, $SiMe_2$), 16.6 (s, 3H, C_5Me_4), 27.3 (s, 3H, C_5Me_4), 27.8 (s, 3H, C_5Me_4), 35.7 (s, 3H, C_5Me_4), 41.0 (d, $^2J_{HH}$ = 9.60 Hz, 1H, CH_2), 51.0 (d, $^2J_{HH}$ = 9.60 Hz, 1H, CH_2). ^{13}C NMR (toluene-d_8): δ −50.0 ($SiMe_2$), −22.4 (N^tBu), −1.4 ($SiMe_2$), 0.1 (C_5Me_4), 1.6 (C_5Me_4), 2.7 (N^tBu), 7.2 ($SiMe_2$), 14.5 ($SiMe_2$), 14.8 (C_5Me_4), 16.5 (C_5Me_4), 19.9 (C_5Me_4), 25.8 (C_5Me_4), 30.7 (C_5Me_4), 39.1 (CH_2), 41.4 (C_5Me_4). IR: 2975 s, 2952 s, 2899 s, 2721 w, 1532 m, 1461 m, 1388 m, 1358 m, 1325 m, 1248 s, 1191 s, 1143 m, 1117 m, 1083 w, 1017 m, 992 w, 902 w, 829 vs, 783 m, 751 m, 730 m, 677 m, 648 w, 590 w cm^{-1}. Anal. Calcd for $C_{34}H_{58}N_2Si_2U$: C, 51.75; H, 7.41; N, 3.55. Found: C, 52.09; H, 7.48; N, 3.45. The resonances of the formimidoyl proton and the methine could not be located, which is typical for protons on carbon atoms directly bound to paramagnetic uranium.

X-ray Crystallographic Data Collection. Table 1 provides information on the X-ray data collection, structure determination, and refinement for **2**, **4**, **5**, and **7**. Additional details are provided in the Supporting Information.

RESULTS

Reactivity of 1 with S_8. Complex **1** reacts with elemental sulfur to produce an orange microcrystalline solid, **2**, that was characterized by NMR and IR spectroscopy and elemental analysis. Complex **2** contains two additional resonances in the ^{1}H NMR spectrum compared to that of **1**, which is consistent with insertion, since it moves the CH_2 groups previously bound directly to uranium further away from the paramagnetic center, allowing them to be observed.[10,18] The X-ray crystal structure of **2** (Figure 1) shows that two sulfur atoms have

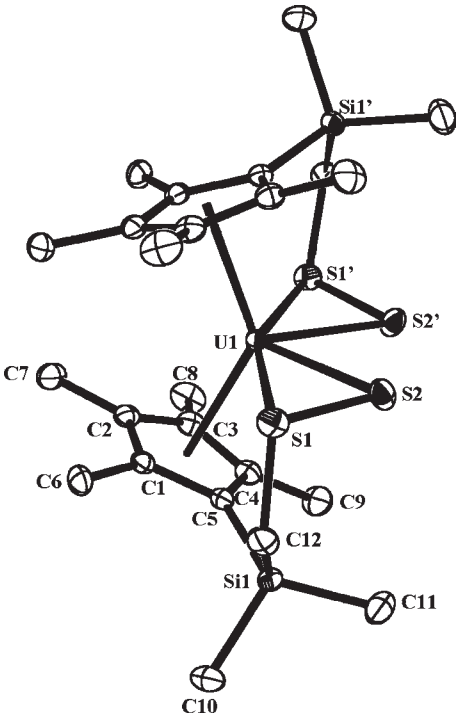

Figure 1. Thermal ellipsoid plot of $(\eta^5{:}\eta^2\text{-}C_5Me_4SiMe_2CH_2S_2)_2U$ (**2**), drawn at the 50% probability level with hydrogen atoms omitted for clarity.

dx.doi.org/10.1021/ja109491k | J. Am. Chem. Soc. 2011, 133, 3507–3516

inserted into each U−C bond to form a new type of ligand, namely a tethered (tetramethylcyclopentadienyl)dimethylsilyl alkyl disulfide, in the complex $(\eta^5{:}\eta^2\text{-}C_5Me_4SiMe_2CH_2S_2)_2U$ (**2**) (eq 3).

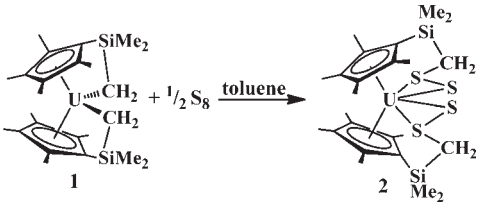

(3)

The ^{1}H NMR spectrum of **2** at −45 °C gave the pattern expected on the basis of the solid-state structure shown in Figure 1. However, the room-temperature spectrum contained more resonances than expected, and the resonances were broader than those commonly found for U^{4+} complexes employing the $(C_5Me_4SiMe_2CH_2)^{2-}$ ligand: 50−200 Hz for **2** versus 5−30 Hz, typically.[10] These differences suggest that there is some fluxionality in the structure of **2** in solution. Similar fluxional characteristics were observed with $[U(N^tBu)_2(I)(^tBu_2bpy)]_2(\mu\text{-}\eta^2{:}\eta^2\text{-}S_4)$ ($^tBu_2bpy$ =4,4′-di-*tert*-butyl-2,2′-bipyridyl).[14] Due to the instability of **2** in solution at room temperature, high-temperature NMR spectra could not be obtained.

Reactivity of 1 with ^{i}PrN=C=N^{i}Pr. Complex **1** reacts with ^{i}PrN=C=N^{i}Pr to form a single product, **3**, which gives a ^{1}H NMR spectrum with a larger number of resonances than expected in comparison to the previously characterized double-insertion products with this system.[10,18] This is consistent with insertion into one of the U−C bonds of **1**, which results in a loss of symmetry between the two cyclopentadienyl rings. Elemental analysis was also consistent with the insertion of 1 equiv of ^{i}PrN=C=N^{i}Pr, and X-ray crystallography revealed that this was indeed a monoinsertion product, the tethered amidinate complex $(\eta^5\text{-}C_5Me_4SiMe_2CH_2\text{-}\kappa C)U[\eta^5\text{-}C_5Me_4SiMe_2CH_2C(^iPrN)_2\text{-}\kappa^2N,N']$ (**3**) (eq 4, Figure 2). Low-temperature NMR studies showed that the broad resonances recorded at room temperature sharpen to give a spectrum consistent with the structure shown in Figure 2, suggesting that **3** is fluxional at room temperature.

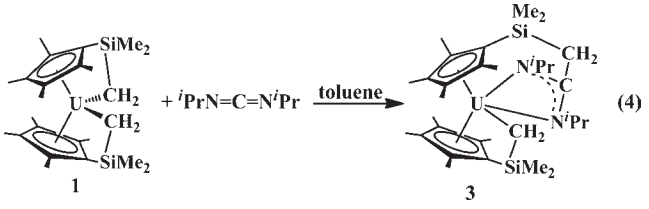

(4)

Although the X-ray data could establish the connectivity of atoms in **3**, it was not of sufficient quality to discuss metrical parameters. To the best of our knowledge, the only other example of an f element complex containing a tethered amidinate ligand is a recently reported complex derived from a metalated $[N(SiMe_3)_2]^-$ ligand, $(Tp^{Me2})Er[(CyN)_2CCH_2SiMe_2N(SiMe_3)]$, where Tp^{Me2} = tris(2,4-dimethylpyrazolyl)borate.[19]

Reactivity of 3 with CO. Complex **3** was of interest for further studies, since it has two different tethered ligands. Comparison of its CO reactivity with that of **1** in eq 1 would probe how the CO insertion is affected by an adjacent amidinate tether. If there is no effect, single insertion into the tethered U−C bond would result in a complex containing both a tethered

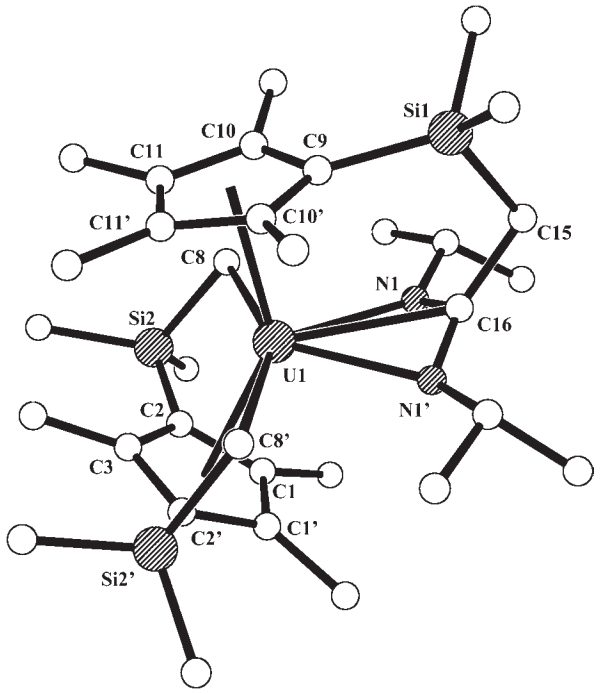

Figure 2. Ball and stick model of $(\eta^5\text{-}C_5Me_4SiMe_2CH_2\text{-}\kappa C)U[\eta^5\text{-}C_5Me_4SiMe_2CH_2C(^iPrN)_2\text{-}\kappa^2N,N']$ (**3**), with Si(2) shown disordered over two positions.

alkoxide and a tethered amidinate. The surprising result of the CO reaction with **3** is shown in eq 5.

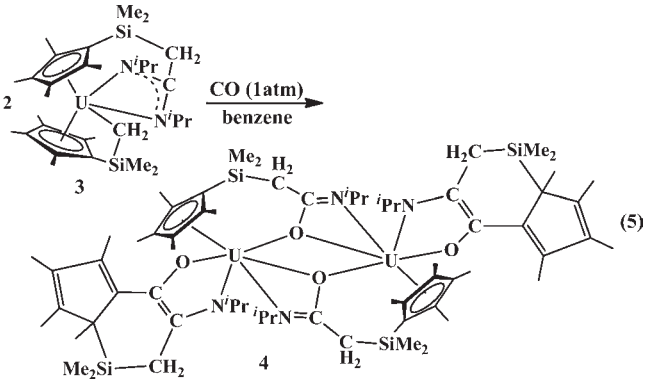

(5)

Complex **3** reacts with CO at 1 atm within 15 min to produce $\{\mu\text{-}[\eta^5\text{-}C_5Me_4SiMe_2CH_2C(=N^iPr)O\text{-}\kappa^2O,N]U[OC(C_5Me_4SiMe_2CH_2)CN(^iPr)\text{-}\kappa^2O,N]\}_2$ (**4**). Complex **4** was characterized by spectroscopic and analytical techniques and was definitively identified by X-ray crystallography (Figure 3). The ^{1}H NMR spectrum of **4** has many resonances, as expected for such a complicated compound, but the NMR of the single crystals examined by X-ray diffraction matched that of the crude powder initially isolated: i.e., complex **4** is formed almost exclusively in this reaction. In further support of the sole formation of **4** in this reaction, elemental analysis of the crude material obtained matched the formula of **4**.

The metrical parameters of **4** described in Structure Analysis are consistent with the resonance structure shown in eq 5. Although this structural analysis is straightforward, the route by which **4** is formed is not. Minimally, the U−CH_2(tether) bond has been cleaved, as well as a C−N linkage in the amidinate ligand. One η^5-cyclopentadienyl ligand has been removed per metal, and one substituent on that ring, either a methyl or a silyl,

dx.doi.org/10.1021/ja109491k |*J. Am. Chem. Soc.* 2011, 133, 3507–3516

has migrated. Newly formed bonds include U−O, C−C, C═C, and C═N. With so many bond cleavage and bond formation processes occurring within the 15 min allowed to generate **4**, it is difficult to suggest, much less identify, a single reaction sequence to form this product. However, a series of reactions can be listed that lead to the observed product. These are described in the next three paragraphs and in Schemes 1 and 2, which show a possible sequence to demonstrate that viable pathways exist.

The μ-[η^5-$C_5Me_4SiMe_2CH_2C(=N^iPr)O$-$\kappa^2O,N$]$^{2-}$ ligand that bridges the two uranium centers in **4** could be generated in the following way. It seems likely that CO insertion into the U−CH_2(tethered) bond could initially occur on the basis of the reactivity shown in eq 1. This would form a U−C(═O)R acyl that would be expected to rearrange to generate a strong U−O interaction, leaving the carbon of the inserted CO with reactive carbene- or carbenium-like character.[20] The reactivity of such species is well-known,[20−27] and the silyl migration that accompanies CO insertion in eq 1 is one example.[10] In eq 5, this carbene intermediate could interact with the proximal tethered amidinate to form a linkage between the inserted carbon of CO and an N^{i}Pr component of the amidinate ligand. This requires a rather remarkable C−N amidinate bond cleavage. Although amidinate cleavage has been found in a small number of transition-metal complexes, such as {[PhC(NSiMe$_3$)$_2$]Zr(η^2-PhCNSiMe$_3$)-(μ-NSiMe$_3$)}$_2$,[28] more extreme conditions of thermolysis[29,30] or reduction[28,31−33] are required. To our knowledge, C−N amidinate bond cleavage has not been previously observed due to insertion of a substrate. Reported examples of amidinate ligand cleavage typically result in the formation of metal−imido[28,29,31,32] or metal−amide[30] bonds, and in only one case[33] did the formation of a new carbon−nitrogen double bond occur as observed in **4**.

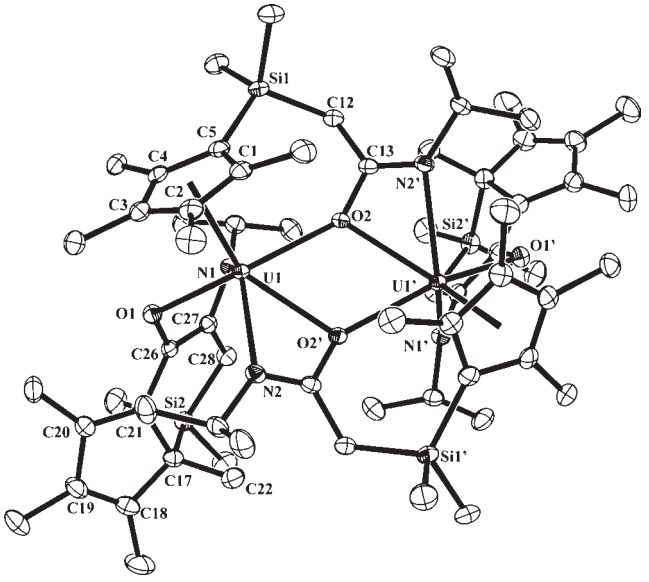

Figure 3. Thermal ellipsoid plot of {μ-[η^5-$C_5Me_4SiMe_2CH_2C(=N^iPr)$-O-$\kappa^2O,N$]U[OC($C_5Me_4SiMe_2CH_2$)CN(^{i}Pr)-$\kappa^2O,N$]}$_2$ (**4**), drawn at the 50% probability level with hydrogen atoms omitted for clarity.

The other ligand present in **4**, the [OC($C_5Me_4SiMe_2CH_2$)-CN(^{i}Pr)-κ^2O,N]$^{2-}$ unit, contains a second CO that has formally inserted. In this case, however, the carbon atom of the CO, C26, is connected to the central carbon atom of the cleaved amidinate, C27, as well as a cyclopentadienyl ring carbon, C21. Since this ring carbon is now bound only to the CO-derived carbon atom, it has lost either a methyl group or the silyl substituent by a rearrangement. One of the ring carbons, C17, has both methyl and silyl groups and the five-membered ring has a localized diene structure. These bonding arrangements leave N1 with only two substituents, and it forms a single bond to uranium.

A speculative route to this nonbridging ligand is shown in Scheme 2. If the formation of the bridging ligand in **4** caused steric crowding (see Scheme 1), it is possible that the other cyclopentadienyl ring could adopt an η^1 coordination mode via the carbon with the most distant substituent, the silyl group. CO insertion into that U−C σ bond would again make a reactive acyl with a carbenium-like carbon atom.[20] Combination of this carbon with the central carbon of the amidinate that has lost an N^{i}Pr group to the bridging ligand (see Scheme 1) would generate the C═C bond observed in the product. Silyl and double-bond migration would put the C═C bonds in conjugation and lead to the nonbridged ligand in **4**.

Scheme 1. Possible Pathway to the Formation of the Bridging Ligand μ-[η^5-$C_5Me_4SiMe_2CH_2C(=N^iPr)O$-$\kappa^2O,N$]$^{2-}$ in 4

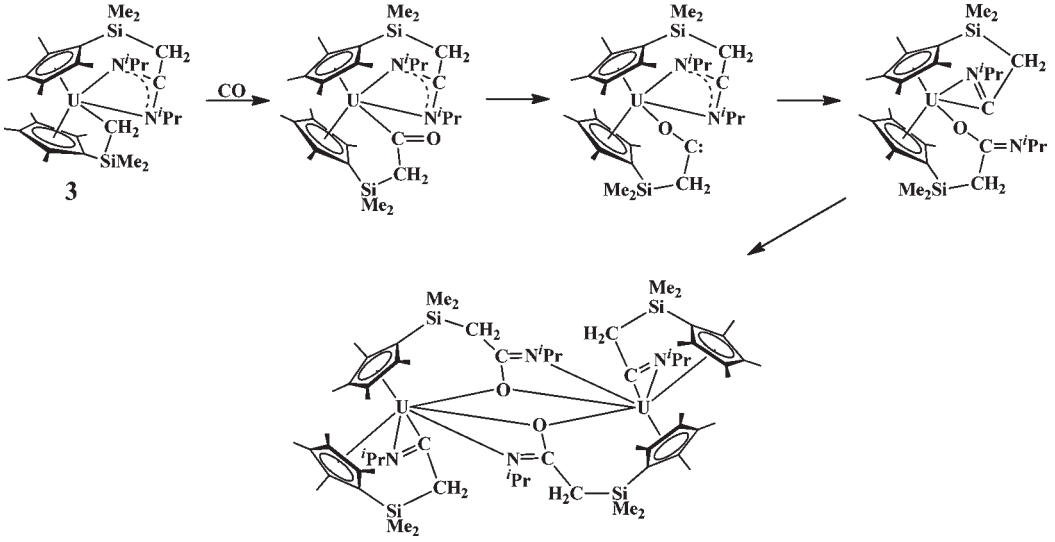

dx.doi.org/10.1021/ja109491k |J. Am. Chem. Soc. 2011, 133, 3507–3516

Scheme 2. Possible Route to the Nonbridging Ligand $[OC(C_5Me_4SiMe_2CH_2)CN(^iPr)\text{-}\kappa^2O,N]^{2-}$ in 4[a]

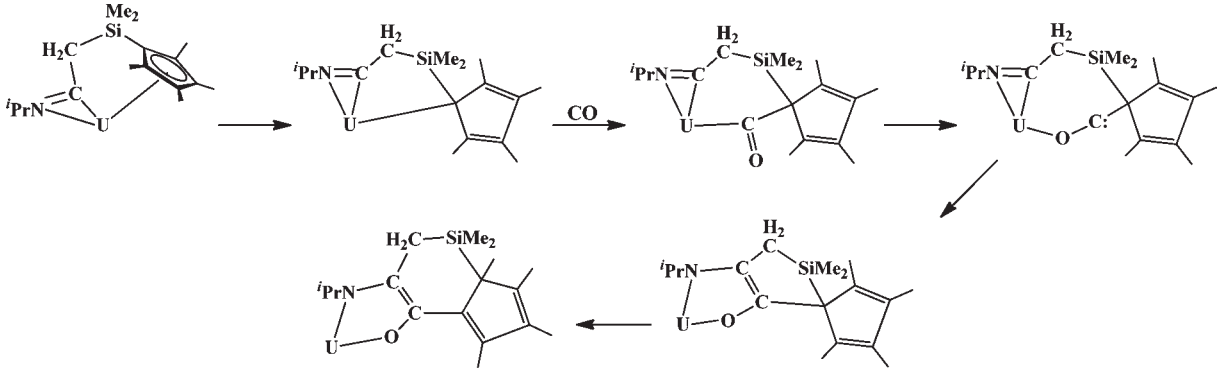

[a] The μ-$[\eta^5\text{-}C_5Me_4SiMe_2CH_2C(=N^iPr)O\text{-}\kappa^2O,N]^{2-}$ ligand and dimeric structure are omitted for clarity.

It is remarkable for such a cascade of reactions to occur at room temperature. Other complicated organouranium multistep reactions are rare. Recently, cascade reactivity have been reported from $[1,1'\text{-fc}(NSi^tBuMe_2)_2]U(CH_2Ph)_2$ with aromatic heterocycles,[34,35] but these require either harsh conditions, e.g. 100 °C for 45 h,[34] or long reaction times to come to completion.[35]

Reactivity of 3 with ^{t}BuN≡C. To make an isoelectronic comparison of the CO reaction in eq 5 and to attempt to isolate an analogue of an intermediate leading to **4**, complex **3** was treated with ^{t}BuN≡C. One equivalent of ^{t}BuN≡C reacts with **3** to generate the monoinsertion product $[\eta^5{:}\eta^2\text{-}C_5Me_4SiMe_2CH_2C(=N^tBu)]U[\eta^5\text{-}C_5Me_4SiMe_2CH_2C(=N^iPr)N(^iPr)\text{-}\kappa N]$ (**5**), which was characterized with standard techniques and was definitively identified with X-ray crystallography (eq 6, Figure 4). This reaction did not lead to the complicated cascade of reactions found in eq 5, but the monoinsertion product contained an amidinate bound to uranium as a tethered monodentate amide in the ligand $[\eta^5\text{-}C_5Me_4SiMe_2CH_2C(=N^iPr)N^iPr\text{-}\kappa N]^{2-}$. This contrasts with the usual κ^2 binding mode of amidinates to metals. This transformation can be rationalized as a result of the increased steric bulk introduced into the coordination environment by forming the tethered iminoacyl ligand $[\eta^5{:}\eta^5\text{-}C_5Me_4SiMe_2CH_2C(=N^tBu)]^{2-}$. This change in binding mode of the amidinate ligand has not been previously reported in the literature, to the best of our knowledge. There are reports of amidinate ligands binding κ^1 to a metal, but these examples are the result of using bulky linked amidinates that bind this way upon complexation.[36,37] The most closely related example in the literature is $[PhC(NSiMe_3)_2]_2Ti(\mu\text{-}O)_2TiL[\eta^1\text{-}NC(Ph)N(SiMe_3)_2]$.[38]

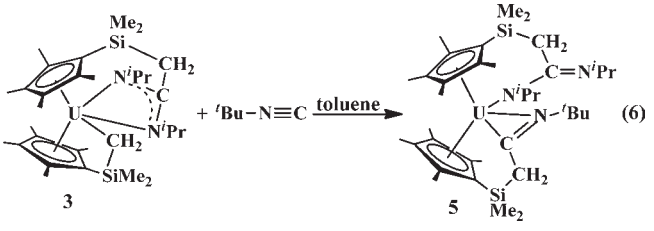

Isomerization of $[\eta^5{:}\eta^2\text{-}C_5Me_4SiMe_2CH_2C(=N^tBu)]_2U$ (6). To further explore the possible effects of steric congestion of tethered iminoacyl ligands that led to the formation of **5** in eq 6, the chemistry of the bis(tethered iminoacyl) complex $[\eta^5{:}\eta^2\text{-}C_5Me_4SiMe_2CH_2C(=N^tBu)]_2U$ (**6**) was examined. The thermal behavior of **6** was examined for this reason and for comparison with the reactivity found in eq 2. Heating a toluene solution of **6** at 110 °C for 12 h led to the formation of $[\eta^5{:}\eta^5{:}\eta^3\text{-}^t\text{BuNC}(CH_2SiMe_2C_5Me_4)(CHSiMe_2C_5Me_4)]U(\eta^2\text{-}HC=N^tBu)$ (**7**) (Figure 5, eq 7).

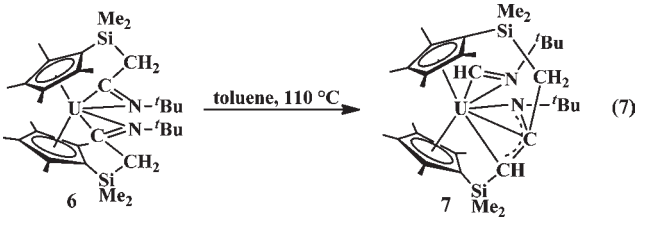

Unlike the reaction shown in eq 2, C−C coupling of the iminoacyl ligands has not occurred in this transformation. Instead, a series of bond-breaking and bond-making events have taken place to form **7**. A C−C bond cleavage has occurred between the carbon of the methylene group of an η^5-$C_5Me_4SiMe_2CH_2$ unit and the carbon of an originally inserted isocyanide. The latter carbon has gained a hydrogen to create a new C−H bond to form a formimidoyl ligand, $(HC=N^tBu)^-$, the first example in actinide chemistry.[39,40] The methylene carbon of the

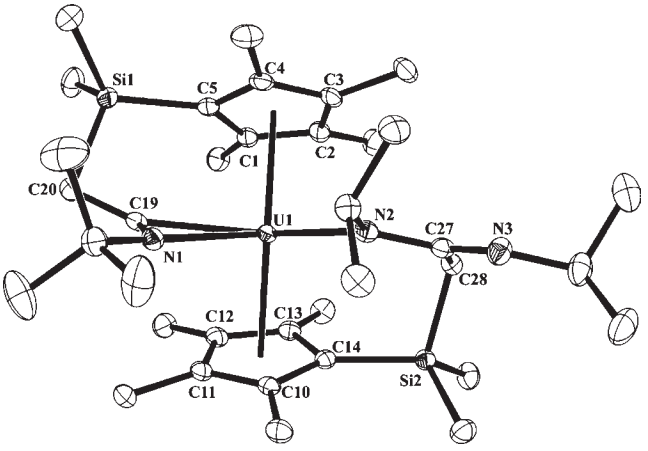

Figure 4. Thermal ellipsoid plot of $[\eta^5{:}\eta^2\text{-}C_5Me_4SiMe_2CH_2C(=N^tBu)]U[\eta^5\text{-}C_5Me_4SiMe_2CH_2C(=N^iPr)N(^iPr)\text{-}\kappa N]$ (**5**), drawn at the 50% probability level with hydrogen atoms omitted for clarity.

dx.doi.org/10.1021/ja109491k | J. Am. Chem. Soc. 2011, 133, 3507–3516

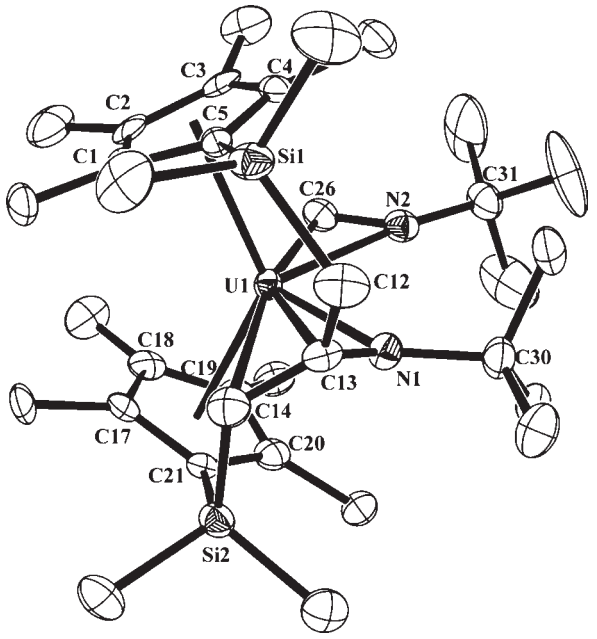

Figure 5. Thermal ellipsoid plot of $[\eta^5{:}\eta^5{:}\eta^3$-^{t}BuNC$(CH_2SiMe_2C_5Me_4)$-$(CHSiMe_2C_5Me_4])U(\eta^2$-HC═N^{t}Bu) (**7**), drawn at the 50% probability level with hydrogen atoms omitted for clarity.

other η^5-$C_5Me_4SiMe_2CH_2$ unit has lost a hydrogen, formally the source of hydrogen for the formimidoyl ligand, and both tethers are attached to the carbon of an originally inserted isocyanide through a newly formed C−C bond. This results in a doubly tethered bis(cyclopentadienyl) trianionic ligand, $[\eta^5{:}\eta^5{:}\eta^3$-^{t}BuNC$(CH_2SiMe_2C_5Me_4)(CHSiMe_2C_5Me_4)]^{3-}$.

Structural Analysis. *$(\eta^5{:}\eta^2$-$C_5Me_4SiMe_2CH_2S_2)_2U$ (**2**).* The metrical parameters of the metallocene part of **2** (Table 2) are similar to those observed for **1**[10] and related compounds.[18] However, **2** differs from products of double insertion with **1** in that the 72.61(3)° S2−U−S2′ bond angle is much smaller than other (donor atom)−U−(donor atom) bond angles such as the 93.15(5)° N−U−N angle in **6**, which also contains $\eta^5{:}\eta^2$-bound ligands,[5] and the 110.06(7)° analogue in $[\eta^5$-$C_5Me_4SiMe_2$-$CH_2C(^t$Bu)N-$\kappa N]_2U$.[18] It is possible that this small angle arises due to weak interactions between S2 and S2′, since the 3.188 Å S2···S2′ distance in **2** is within the sum of the van der Waals radii of 3.7 Å.[41]

Interestingly, it is the S2 position that forms the primary contact with uranium, with a U−S2 bond distance of 2.6924(6) Å versus 2.9572(6) Å for U−S1. The U−S2 distance is similar to the 2.708(2) and 2.639(4) Å U−S terminal ligand bond lengths found in $(C_5Me_5)_2UMe(SPh)$[42] and $(C_5Me_5)_2U(SMe)_2$,[43] respectively, as well as the 2.711(3) Å U−S bond in the side-on-bound $(\eta^2$-$S_2)^{2-}$ sulfide complex $[Pr_2NH_2]_2\{UO_2(\eta^2$-$S_2)[O(S)$-$CNPr_2$-$\kappa^2O,S]_2\}$ (**8**).[44] The $[O(S)CNPr_2$-$\kappa^2O,S]^-$ ligand in **8** is similar in that the primary connection involves the 2.476(6) Å U−O bond and the U−S bond is 2.873(2) Å.[44] The 2.0503(9) Å S1−S2 bond distance in **2** matches the 2.05(1) Å S−S bond distance of the $(\eta^2$-$S_2)^{2-}$ ligand in **8**[44] and is a typical distance for an S−S bond.[45]

*$\{\mu$-$[\eta^5$-$C_5Me_4SiMe_2CH_2C(═N^iPr)O$-$\kappa^2O,N]U[OC(C_5Me_4SiMe_2$-$CH_2)CN(^iPr)$-$\kappa^2O,N]\}_2$ (**4**).* In the structure of **4**, the 1.291(3) Å C13−N2′, 1.351(3) Å C18−C19, 1.362(3) Å C20−C21, and 1.380(3) Å C26−C27 bond distances (Table 3) are all within the double-bond range.[45] The other C−C, C−O, and C−N bonds are all consistent with single bonds.[45] The 2.509 Å U−(cyclopentadienyl centroid) distance in **4** is similar to those in other $(C_5Me_4SiMe_2X)^{2-}$ complexes: 2.419 Å in **1** (X = CH_2),[10] 2.498 Å in **2** (X = S_2), and 2.524 Å in **6** (X = CN^{t}Bu).[10] The 2.206(2) Å U−N1 bond distance is within the reported range of U−NR_2 amide bonds,[46] and the 2.579(2) Å U−N2 bond distance matches those found for U←:NR_3 uranium−amine linkages.[47,48] The 2.179(1) Å U−O1 bond is longer than those typically reported for terminal alkoxides, such as the 2.05(1) Å U−O bond length reported for $[(C_5Me_5)_2U$-$(OMe)]_2PH$.[49] However, a longer U−O distance, 2.132(2) Å, was also observed in $(\eta^5$-$C_5Me_4SiMe_2C(=CH_2)O$-$\kappa O)_2U$, **9**, eq 1,[10] which is also a tethered alkoxide similar to **4**. Complexes **4** and **9** also contain significantly bent U−O−C bond angles: 143.4(1)° for U1−O2−C13 and 100.6(1)° for U1−O1−C26 in **4**, and 135.5° in **9**,[10] compared to the typical range for terminal alkoxides of 170.2(5)° to 178(1)°.[49−52] This atypical bond angle can be attributed to the tethered nature of the ligand.[10] The 2.481(1) and 2.518(1) Å U−O2 and U−O2′ distances, respectively, are typical of those observed for bridging alkoxide ligands.[52]

*$[\eta^5{:}\eta^2$-$C_5Me_4SiMe_2CH_2C(═N^tBu)]U[\eta^5$-$C_5Me_4SiMe_2CH_2C$-$(═N^iPr)N(^iPr)$-$\kappa N]$ (**5**).* The structural parameters for **5** (Table 4) are similar to those of $[\eta^5{:}\eta^2$-$C_5Me_4SiMe_2CH_2C(═N^tBu)]_2U$ (**6**), which also contains tethered iminoacyl ligands.[10] For example, the U−(centroid) distances of 2.521 and 2.514 Å in **5** are very similar to the 2.524 and 2.531 Å distances in **6**. The iminoacyl ligand of **5** has the same 1.281(2) Å C−N bond distance as in **6** within experimental error. The iminoacyl ligand in **5** also has similar U−C and U−N bond distances of 2.362(2) and 2.503(2) Å, respectively, compared to the 2.385(2) and 2.397(2) Å U−C and the 2.489(2) and 2.481(2) Å U−N bonds in **6**. The 2.350(2) Å U−N(amide) bond distance is typical of previously reported uranium amide metallocenes, such as the 2.29(1) Å U−N bond distance in $(C_5H_5)_3UN(C_6H_5)_2$.[53]

*$[\eta^5{:}\eta^3$-^{t}BuNC$(CH_2SiMe_2C_5Me_4)(CHSiMe_2C_5Me_4)]U(\eta^2$-$HC═N^tBu)$ (**7**).* Metrical details on the structure of **7** are given in Table 5. The similarity of the 2.532 and 2.551 Å U−(ring centroid) distances and the 130.9° (ring centroid)−U−(ring centroid) angle in **7** with those in **1** and **5** indicate that the cyclopentadienyl parts of the double-tethered trianionic ligand can ligate uranium much like two individually tethered cyclopentadienyl rings. The $(\eta^3$N,C,C′$)^-$ part of the trianion is

Table 2. Selected Bond Distances (Å) and Angles (deg) for $(\eta^5{:}\eta^2$-$C_5Me_4SiMe_2CH_2S_2)_2U$ (2)

Bond Distances	
U1−$(C1-C5)_{centroid}$	2.498
U1−S1	2.9572(6)
U1−S2	2.6924(6)
S1−S2	2.0503(9)
S1−C12	1.813(3)
Bond Angles	
$(C1-C5)_{centroid}$−U1−$(C1'-C5')_{centroid}$	133.3
$(C1-C5)_{centroid}$−U1−S1	96.0
$(C1-C5)_{centroid}$−U1−S2	111.2
S2−U1−S2′	72.61(3)
Contact Distance	
S2···S2′	3.188

dx.doi.org/10.1021/ja109491k |*J. Am. Chem. Soc.* 2011, 133, 3507–3516

attached to uranium primarily through the nitrogen, with a U−N1 distance of 2.368(5) Å similar to the 2.350(2) Å U−N length in **5**. In comparison, the 2.878(5) Å U−C13 and 2.988(6) Å U−C14 distances are significantly longer. A C(14)=C(13)−N^{t}Bu resonance structure would fit with these uranium distances, but the 1.368(7) Å C13−C14 bond distance is longer than a typical C=C bond.[45] This, along with the 1.366(7) Å N1−C13 bond distance, which is shorter than a typical C−N bond,[45] suggests some delocalization.

Formimidoyl ligands in f element complexes are rare, and no examples of actinide formimidoyl complexes were previously known. The $[(C_5H_5)_2Ln(\mu,\eta^2\text{-}HC{=}N^tBu)]_2$ complexes of yttrium (**10**)[39] and erbium (**11**)[40] have metal−formimidoyl parameters that differ from those of **7**, most likely due to the terminal versus bridging modes. The 1.252(7) Å N2−C26 bond distance in **7** is similar, within experimental error, to the analogous bond lengths in **10** and **11**, 1.275(6) and 1.262(8) Å, respectively. The 2.343(6) Å M−C and 2.575(5) Å M−N distances in **7** are very different than those of **10**, 2.545(5) and 2.325(4) Å, and **11**, 2.527(6) and 2.312(5) Å, respectively. The formimidoyl ligand is clearly bound to uranium primarily through carbon rather than nitrogen.

Table 3. Selected Bond Distances (Å) and Angles (deg) for $\{\mu\text{-}[\eta^5\text{-}C_5Me_4SiMe_2CH_2C(=N^iPr)O\text{-}\kappa^2O,N]U[OC(C_5Me_4SiMe_2CH_2)CN(^iPr)\text{-}\kappa^2O,N]\}_2$ (4)

Bond Distances			
U1−(C1−C5)$_{centroid}$	2.509	C26−C27	1.380(3)
U1−N1	2.206(2)	C13−O2	1.330(2)
U1−N2	2.579(2)	N1−C27	1.405(2)
U1−O1	2.179(1)	C17−C18	1.491(3)
U1−O2	2.481(1)	C19−C20	1.462(3)
U1−O2′	2.518(1)	C21−C26	1.475(3)
C13−N2′	1.291(3)	C26−O1	1.360(1)
C18−C19	1.351(3)	C27−C28	1.519(3)
C20−C21	1.362(3)		
Bond Angles			
(C$_1$−C$_5$)$_{centroid}$−U1−N1	115.8	N2−U1−O1	82.30(5)
(C$_1$−C$_5$)$_{centroid}$−U1−N2	112.0	N2−U1−O2	110.62(5)
(C$_1$−C$_5$)$_{centroid}$−U1−-O1	92.4	N2−U1−O2′	51.50(5)
(C$_1$−C$_5$)$_{centroid}$−U1−O2	96.9	O1−U1−O2	159.59(5)
(C$_1$−C$_5$)$_{centroid}$−U1−O2′	133.6	O1−U1−O2′	121.66(5)
N1−U1−N2	126.61(6)	O2−U1−O2′	62.62(5)
N1−U1−O1	73.55(6)	U1−O2−C13	143.4(1)
N1−U1−O2	86.03(5)	U1−O1−C26	100.6(1)
N1−U1−O2′	104.44(5)		

DISCUSSION

The formation of $(\eta^5{:}\eta^2\text{-}C_5Me_4SiMe_2CH_2S_2)_2U$ (**2**) (eq 3) represents the first example of insertion of elemental sulfur into a U−C bond, and it provides the first f element complex with an alkyl disulfide ligand. Alkyl disulfide ligands from sulfur insertion are known with W[54] and Ga,[55] but in general they are rare.[56,57] In the past, organoactinide complexes of alkyl sulfides have been made primarily from RSH,[58−60] RSM (M = alkali metal),[61−63] CS_2 insertion,[43] and RSSR substrates.[42,43,64,65] To our knowledge, there is only a single example of the use of S_8 as a reagent in organoactinide chemistry in the formation of $[U(N^tBu)_2(I)(^tBu_2bpy)]_2(\mu,\eta^2{:}\eta^2\text{-}S_4)$ from $[U(N^tBu)_2(I)(^tBu_2bpy)]_2$.[14] Insertion of sulfur into lanthanide−alkyl bonds using S_8 is known with organolanthanides such as $[(C_5H_4R)_2LnR']_x$,[66,67] where R = H, $SiMe_2{}^tBu$ and R′ = Me, *n*-Bu. The closest related organoactinide polysulfide to **2** in the literature is $(C_5Me_5)_2ThS_5$, made from $(C_5Me_5)_2ThCl_2$ and Li_2S_5.[62] Clearly, the use of S_8 as a substrate should be more widely explored.

The formation of $(\eta^5\text{-}C_5Me_4SiMe_2CH_2\text{-}\kappa C)U[\eta^5\text{-}C_5Me_4SiMe_2CH_2C(^iPrN)_2\text{-}\kappa^2N,N']$ (**3**) from **1** by carbodiimide insertion (eq 4) is conventional, but the subsequent reactivity of **3** with CO (eq 5) was unexpected. It is well-known that CO can insert into metal−alkyl bonds of electropositive metals to generate reactive carbon species,[20] but the cascade of reactions leading to the isolation of $\{\mu\text{-}[\eta^5\text{-}C_5Me_4SiMe_2CH_2C(=N^iPr)\text{-}O\text{-}\kappa^2O,N]U[OC(C_5Me_4SiMe_2CH_2)CN(^iPr)\text{-}\kappa^2O,N]\}_2$ (**4**) is unprecedented. Diaconescu and co-workers have recently reported two examples of cascade reactions arising from a uranium bis(benzyl) complex,[34,35] but in general such cascade reactions are rare for organoactinides. The fact that addition of just CO at room temperature can trigger the transformation of **3** to **4** demonstrates that there is much inherent reactivity available from U−C bonds in the proper coordination environment. Although the sequence of individual steps in the **3** to **4** conversion are unknown, the overall reaction demonstrates the extensive amount of bond making and bond breaking that can be accessed via properly positioned U−C bonds.

The reaction of **3** with isoelectronic ^{t}BuN≡C to generate $[\eta^5{:}\eta^2\text{-}C_5Me_4SiMe_2CH_2C(=N^tBu)]U[\eta^5\text{-}C_5Me_4SiMe_2CH_2C(=N^iPr)N(^iPr)\text{-}\kappa N]$ (**5**) (eq 6) shows that the reactivity of **3** can be controlled to avoid the massive restructuring that occurs in the CO reaction (eq 5). The reaction also shows how insertion and tethering can power a rare example of an amidinate

Table 4. Selected Bond Distances (Å) and Angles (deg) for $[\eta^5{:}\eta^2\text{-}C_5Me_4SiMe_2CH_2C(=N^tBu)]U[\eta^5\text{-}C_5Me_4SiMe_2CH_2C(=N^iPr)N(^iPr)\text{-}\kappa N]$ (5)

Bond Distances			
U1−(C1−C5)$_{centroid}$	2.521	U1−N2	2.350(2)
U1−(C10−C14)$_{centroid}$	2.514	C19−N1	1.281(2)
U1−C19	2.362(2)	C27−N2	1.386(2)
U1−N1	2.503(2)	C27−N3	1.287(2)
Bond Angles			
(C1−C5)$_{centroid}$−U1−(C10−C14)$_{centroid}$	131.3	(C1−C5)$_{centroid}$−U1−N2	103.8
(C1−C5)$_{centroid}$−U1−C19	91.9	N1−U1−N2	97.67(5)
(C1−C5)$_{centroid}$−U1−N1	109.5		

dx.doi.org/10.1021/ja109491k |*J. Am. Chem. Soc.* 2011, 133, 3507–3516

Table 5. Selected Bond Distances (Å) and Angles (deg) for $[\eta^5{:}\eta^5{:}\eta^3\text{-}^t\text{BuNC}(CH_2SiMe_2C_5Me_4)(CHSiMe_2C_5Me_4)]U(\eta^2\text{-}HC{=}N^tBu)$ (7)

Bond Distances			
U−(C1−C5)$_{centroid}$	2.551	U−C26	2.343(6)
U−(C17−C21)$_{centroid}$	2.532	N1−C13	1.366(7)
U−N1	2.368(5)	C13−C14	1.368(7)
U−C13	2.878(5)	N2−C26	1.252(7)
U−C14	2.988(6)	C12−C13	1.504(7)
U−N2	2.575(5)	Si2−C14	1.866(6)
Bond Angles			
(C1−C5)$_{centroid}$−U−(C17−C21)$_{centroid}$	130.9	N1−C14−C13	117.5(5)
N1−U1−N2	91.51(2)		

rearrangement. It is possible that this rearrangement is a key intermediate to the formation of **4**, as it is expected that CO would initially insert into the U−C bond of **3** to form a tethered η^2-acyl, analogous to the tethered η^2-iminoacyl in **5**. The bulk of this η^2-acyl around the metal center could force the amidinate binding mode to change. The possibility of **5** being an analogue of an intermediate in the formation of **4**, as well as the importance of the tether in this reactivity, are supported by the fact that eq 6 contrasts significantly with the reactivity of an analogous untethered bis(pentamethylcyclopentadienyl) methyl uranium amidinate, $(C_5Me_5)_2UMe[(^i\text{Pr})NC(Me)N(^i\text{Pr})\text{-}\kappa^2N,N']$ (**12**).[15] Complex **12** shows significantly reduced reactivity of the U−C(Me) bond and no tendency to rearrange the amidinate when combined with a variety of reagents,[68,69] including ^{t}Bu-N≡C, for which no reaction with **12** was observed. Complex **12** also does not react with CO in a manner analogous to that of **3**, in that after 1 h no reaction was observed. The observed rearrangement to form **5** could be facilitated by tethering either by straining the amidinate−uranium linkage, making rearrangement more energetically favorable, or by providing room for the isocyanide insertion to occur to form the iminoacyl ligand that is bulky enough to drive the amidinate rearrangement.

The isomerization of $[\eta^5{:}\eta^2\text{-}C_5Me_4SiMe_2CH_2C(=N^tBu)]_2U$ (**6**) to $[\eta^5{:}\eta^5{:}\eta^3\text{-}^t\text{BuNC}(CH_2SiMe_2C_5Me_4)(CHSiMe_2C_5Me_4)]\text{-}U(\eta^2\text{-}HC{=}N^tBu)$ (**7**) (eq 7) also demonstrates the reaction potential available via tethering. In this case, alkyl C−H bond activation is occurring with a methylene group that does not appear to be positioned either sterically or electronically to react as it does. It is difficult to imagine how the double-tethered trianion $[\eta^5{:}\eta^5{:}\eta^3\text{-}^t\text{BuNC}(CH_2SiMe_2C_5Me_4)\text{-}(CHSiMe_2C_5Me_4)]^{3-}$ formed in this reaction could be independently made in other ways. Hence, this reaction provides a route to a new type of ligand system as well as the first example of a formimidoyl ligand in organoactinide chemistry. This reaction also provides a new type of reactivity for bis(iminoacyl) metal complexes, which previous to this was well documented to produce endiamido ligands[16] by coupling the iminoacyl ligands (eq 2).[17]

CONCLUSION

This investigation demonstrates that tethering alkyl ligands to cyclopentadienyl rings in uranium complexes can lead to new organoactinide chemistry. Each of the reactions presented here with the $(\eta^5\text{-}C_5Me_4SiMe_2CH_2\text{-}\kappa C)_2U$ system represent previously unobserved types of reactivity for U−C bonds. Equations 5−7 represent new transformations in organometallic chemistry in general.

These results suggest that there is a considerable amount of untapped reaction chemistry available from organoactinides when the appropriate coordination environment is constructed. Tethering may not be the only way to access this reactivity, but as is typical of tethered systems, this approach provides the first evidence that such reactivity is available. In addition to the new reactions, these results have provided new ligand systems. Hence, the uses of the original tethers in **1** have propagated new tethered and double-tethered cyclopentadienyl ligands that may engender new reactivity on their own.

ASSOCIATED CONTENT

Supporting Information. Text, tables, and CIF files giving X-ray data collection, structure determination, refinement, and X-ray diffraction details of compounds **2**, **4**, **5**, and **7**. This material is available free of charge via the Internet at http://pubs.acs.org. CCDC 786120 (**2**), 786121 (**4**), 786122 (**5**), and 786123 (**7**) also contain the supplementary crystallographic data for this paper. These data can be obtained free of charge from The Cambridge Crystallographic Data Centre via www.ccdc.cam.ac.uk/data_request/cif.

AUTHOR INFORMATION

Corresponding Author
wevans@uci.edu

ACKNOWLEDGMENT

We thank the Chemical Sciences, Geosciences, and Biosciences Division of the Office of Basic Energy Sciences of the Department of Energy for support and Dr. Michael K. Takase for assistance with X-ray crystallography.

REFERENCES

(1) Barnea, E.; Eisen, M. S. *Coord. Chem. Rev.* **2006**, *250*, 855.
(2) Castro-Rodriguez, I.; Meyer, K. *Chem. Commun.* **2006**, 1353.
(3) Andrea, T.; Eisen, M. S. *Chem. Soc. Rev.* **2008**, *37*, 550.
(4) Fox, A. R.; Bart, S. C.; Meyer, K.; Cummins, C. C. *Nature* **2008**, *455*, 341.
(5) McDermott, J. X.; White, J. F.; Whitesides, G. M. *J. Am. Chem. Soc.* **1976**, *98*, 6521.
(6) McDermott, J. X.; Wilson, M. E.; Whitesides, G. M. *J. Am. Chem. Soc.* **1976**, *98*, 6529.

(7) Van der Boom, M. E.; Milstein, D. *Chem. Rev.* **2003**, *103*, 1759.
(8) Liddle, S. T.; Edworthy, I. S.; Arnold, P. L. *Chem. Soc. Rev.* **2007**, *36*, 1732.
(9) Stubbert, B. D.; Marks, T. J. *J. Am. Chem. Soc.* **2007**, *129*, 4253.
(10) Evans, W. J.; Siladke, N. A.; Ziller, J. W. *Chem. Eur. J.* **2010**, *16*, 796.
(11) Dormond, A.; Elbouadili, A. A.; Moise, C. *J. Chem. Soc., Chem. Commun* **1984**, 749.
(12) Roger, M.; Belkhiri, L.; Thuéry, P.; Arliguie, T.; Fourmigué, M.; Boucekkine, A.; Ephritikhine, M. *Organometallics* **2005**, *24*, 4940.
(13) Arliguie, T.; Doux, M.; Mézailles, N.; Thuéry, P.; Le Floch, P.; Ephritikhine, M. *Inorg. Chem.* **2006**, *45*, 9907.
(14) Spencer, L. P.; Yang, P.; Scott, B. L.; Batista, E. R.; Boncella, J. M. *Inorg. Chem.* **2009**, *48*, 11615.
(15) Evans, W. J.; Walensky, J. R.; Ziller, J. W.; Rheingold, A. L. *Organometallics* **2009**, *28*, 3350.
(16) Durfee, L. D.; Rothwell, I. P. *Chem. Rev.* **1998**, *88*, 1059.
(17) Kloppenburg, L.; Petersen, J. L. *Organometallics* **1997**, *16*, 3548.
(18) Evans, W. J.; Siladke, N. A.; Ziller, J. W. *C. R. Chim.* **2010**, *13*, 775.
(19) Han, F.; Zhang, J.; Yi, W.; Zhang, Z.; Yu, J.; Weng, L.; Zhou, X. *Inorg. Chem.* **2010**, *49*, 2793.
(20) Tatsumi, K.; Nakamura, A.; Hofmann, P.; Stauffert, P.; Hoffmann, R. *J. Am. Chem. Soc.* **1985**, *107*, 4440.
(21) Manriquez, J. M.; Fagan, P. J.; Marks, T. J.; Day, C. S.; Day, V. W. *J. Am. Chem. Soc.* **1978**, *100*, 7112.
(22) Simpson, S. J.; Andersen, R. A. *J. Am. Chem. Soc.* **1981**, *103*, 4063.
(23) Petersen, J. L.; Egan, J. W. J. *Organometallics* **1987**, *6*, 2007.
(24) Lee, L.; Berg, D. J.; Einstein, F. W.; Batchelor, R. J. *Organometallics* **1997**, *16*, 1819.
(25) Cameron, T. M.; Gordon, J. C.; Scott, B. L.; Tumas, W. *Chem. Commun.* **2004**, 1398.
(26) Berno, P.; Minhas, R.; Hao, S.; Gambarotta, S. *Organometallics* **1994**, *13*, 1052.
(27) Putzer, M. A.; Neumüller, B.; Dehnicke, K. *Z. Anorg. Allg. Chem.* **1998**, *624*, 57.
(28) Hagadorn, J. R.; Arnold, J. *Organometallics* **1994**, *13*, 4670.
(29) Ong, T.; Yap, G. P. A.; Richeson, D. S. *Chem. Commun.* **2003**, 2612.
(30) Flores, J. C.; Chien, J. C. W.; Rausch, M. D. *Organometallics* **1995**, *14*, 1827.
(31) Cotton, F. A.; Wojtczak, W. A. *Polyhedron* **1994**, *13*, 1337.
(32) Cotton, F. A.; Daniels, L. M.; Matonic, J. H.; Wang, X.; Murillo, C. A. *Polyhedron* **1997**, *16*, 1177.
(33) Hagadorn, J. R.; Arnold, J. *J. Am. Chem. Soc.* **1996**, *118*, 893.
(34) Monreal, M. J.; Khan, S.; Diaconescu, P. L. *Angew. Chem., Int. Ed.* **2009**, *48*, 8352.
(35) Duhović, S.; Monreal, M. J.; Diaconescu, P. L. *Inorg. Chem.* **2010**, *49*, 7165.
(36) Bai, S. D.; Tong, H. B.; Guo, J. P.; Zhou, M. S.; Liu, D. S. *Inorg. Chim. Acta* **2009**, *362*, 1143.
(37) Bai, S. D.; Tong, H. B.; Guo, J. P.; Zhou, M. S.; Liu, D. S.; Yung, S. F. *Polyhedron* **2010**, *29*, 262.
(38) Hagadorn, J. R.; Arnold, J. *Organometallics* **1998**, *17*, 1355.
(39) Evans, W. J.; Hanusa, T. P.; Meadows, J. H. *Organometallics* **1987**, *6*, 295.
(40) Evans, W. J.; Meadows, J. H.; Hunter, W. E.; Atwood, J. L. *Organometallics* **1983**, *2*, 1252.
(41) Pauling, L. *The Nature of the Chemical Bond*, 3rd ed.; Cornell University Press: Ithaca, NY, 1960.
(42) Evans, W. J.; Miller, K. A.; Ziller, W. J.; DiPasquale, A. G.; Heroux, K. J.; Rheingold, A. L. *Organometallics* **2007**, *26*, 4287.
(43) Leverd, P. C.; Ephritikhine, M.; Lance, M.; Vigner, J.; Nierlich, M. *J. Organomet. Chem.* **1996**, *507*, 229.
(44) Perry, D. L.; Zalkin, A.; Ruben, H.; Templeton, D. H. *Inorg. Chem.* **1982**, *21*, 237.
(45) Allen, F. H.; Kennard, O.; Watson, D. G. *J. Chem. Soc., Perkin Trans. 2* **1987**, S1.
(46) Jantunen, K. C.; Burns, C. J.; Castro-Rodriguez, I.; Da Re, R. E.; Golden, J. T.; Morris, D. E.; Scott, B. L.; Taw, F. L.; Kiplinger, J. L. *Organometallics* **2004**, *23*, 4682.
(47) Scott, P.; Hitchcock, P. B. *J. Chem. Soc., Dalton Trans.* **1995**, 603.
(48) Eigenbrot, C. W. J.; Raymond, K. N. *Inorg. Chem.* **1982**, *21*, 2653.
(49) Duttera, M. R.; Day, V. W.; Marks, T. J. *J. Am. Chem. Soc.* **1984**, *106*, 2907.
(50) Evans, W. J.; Miller, K. A.; DiPasquale, A. G.; Rheingold, A. L.; Stewart, T. J.; Bau, R. *Angew. Chem., Int. Ed.* **2008**, *47*, 5075.
(51) Boisson, C.; Berthet, J. C.; Lance, M.; Nierlich, M.; Ephritikhine, M. *Chem. Commun.* **1996**, 2129.
(52) Brunelli, M.; Perego, G.; Lugli, G.; Mazzei, A. *J. Chem. Soc., Dalton Trans.* **1979**, 861.
(53) Cramer, R. E.; Engelhardt, U.; Higa, K. T.; Gilje, J. W. *Organometallics* **1987**, *6*, 41.
(54) Legzdins, P.; Rettig, S. J.; Sánchez, L. *Organometallics* **1988**, *7*, 2394.
(55) Shang, G.; Hampden-Smith, M. J.; Duesler, E. N. *Inorg. Chem.* **1996**, *35*, 2611.
(56) Morton, M. S.; Lachicotte, R. J.; Vicic, D. A.; Jones, W. D. *Organometallics* **1999**, *18*, 227.
(57) Shaver, A.; Plouffe, P. Y. *Inorg. Chem.* **1994**, *33*, 4327.
(58) Leverd, P. C.; Lance, M.; Vigner, J.; Nierlich, M.; Ephritikhine, M. *J. Chem. Soc., Dalton Trans.* **1995**, 237.
(59) Leverd, P. C.; Lance, M.; Nierlich, M.; Vigner, J.; Ephritikhine, M. *J. Chem. Soc., Dalton Trans.* **1994**, 3563.
(60) Lin, Z.; Brock, C. P.; Marks, T. J. *Inorg. Chim. Acta* **1988**, *141*, 145.
(61) Leverd, P. C.; Arliguie, T.; Lance, M.; Nierlich, M.; Vigner, J.; Ephritikhine, M. *J. Chem. Soc., Dalton Trans.* **1994**, 501.
(62) Wrobleski, D. A.; Cromer, D. T.; Ortiz, J. V.; Rauchfuss, T. B.; Ryan, R. R.; Sattelberger, A. P. *J. Am. Chem. Soc.* **1986**, *108*, 174.
(63) Jones, R. G.; Karmas, G.; Martin, G. A., Jr.; Gilman, H. *J. Am. Chem. Soc.* **1956**, *78*, 4285.
(64) Gaunt, A. J.; Scott, B. L.; Neu, M. P. *Inorg. Chem.* **2006**, *45*, 7401.
(65) Evans, W. J.; Miller, K. A.; Kozimor, S. A.; Ziller, J. W.; DiPasquale, A. G.; Rheingold, A. L. *Organometallics* **2007**, *26*, 3568.
(66) Zhang, Z.; Li, Y.; Liu, R.; Chen, Z.; Weng, L.; Zhou, X. *Polyhedron* **2007**, *26*, 4986.
(67) Li, Y.; Pi, C.; Zhang, J.; Zhou, X.; Chen, Z.; Weng, L. *Organometallics* **2005**, *24*, 1982.
(68) Evans, W. J.; Walensky, J. R.; Ziller, J. W. *Organometallics* **2010**, *29*, 101.
(69) Evans, W. J.; Walensky, J. R.; Ziller, J. W. *Inorg. Chem.* **2010**, *49*, 1743.